JPE 8-3-4

Intelligent Diagnosis of Broken Bars in Induction Motors Based on New Features in Vibration Spectrum

Alireza Sadoughi*, Mohammad Ebrahimi†, Mehdi Moallem*, Saeid Sadri*

†*Dept. of Electrical and Computer Eng., Isfahan University of Technology, Isfahan, Iran

ABSTRACT

Many induction motor broken bar diagnosis methods are based on evaluating special components in machine signals spectrums. Current, power, flux, etc are among these signals. Frequencies related to a broken rotor fault are slip dependent, therefore, correct diagnosis of fault - especially when obtrusive frequency components are present - depends on accurate determination of motor velocity and slip. The traditional methods typically require several sensors that should be pre-installed in some cases. This paper presents a diagnosis method based on only a vibration sensor. Motor velocity oscillation due to a broken rotor causes frequency components at twice slip frequency difference around speed frequency in vibration spectrum. Speed frequency and its harmonics as well as twice supply frequency, can easily and accurately be found in a vibration spectrum, therefore the motor slip can be computed. Now components related to rotor fault can be found. It is shown that a trained neural network – as a substitute for an expert person – can easily categorize the existence and the severity of a fault according to the features extracted from the presented method. This method requires no information about the motor internal structure and has been able to diagnose correctly in all the laboratory tests.

Keywords: Broken bar, Fault diagnosis, Induction motor, Intelligent, Vibration

1. Introduction

The electrical motors most widely used in industrial applications are three phase squirrel cage induction motors; therefore, prediction of the running conditions and reliability of these motors is crucial to avoid unexpected and catastrophic failures. About 10% of induction motor faults are due to broken rotor bars. Much research has been done on the on-line diagnosis of broken bars and numerous approaches have been introduced in published literature. Reviews about some of these approaches are presented in [1] and [2]. In some references, the application of search coils are proposed to measure the fluxes related to rotor fault [3], [4]. Motor parameter estimation [6], Park's Vector method [9], harmonic analysis of speed fluctuations [5], [6], frequency analysis of instantaneous power [7], [8], and machine current signature analysis (MCSA) [10], [11] are among the proposed methods presented in technical literature. These methods have some drawbacks due to one or more of the following requirements:

- Requiring more than one sensor/ or pre-installed sensors such as search coils or tachometers

Manuscript received Dec. 10, 2007; revised April. 23, 2008
† Corresponding Author: mebrahim@cc.iut.ac.ir
Tel: +98-311-391-5388, Fax: +98-311-391-2451, Isfahan Univ. of Tech.
* Dept. of Elec. and Computer Eng. , Isfahan Univ. of Tech.

- High precision sensors, because measurements obtained by numerous sensors should be combined mathematically. (The errors from different sensors add together to high values.)
- Connection to live electric parts for voltage measurement
- Knowledge of motor internal structure (such as motor slots) for speed estimation

A practical diagnosis method should be easily performed by operators in site and does not take too much time. Among different on-line fault diagnosing methods the most attention is allocated to evaluating certain frequency magnitudes in machine signals spectrums. Current, power, flux, etc are among these signals. Frequencies related to broken rotor faults are dependent on slip; therefore, correct diagnosis of a fault depends on the accurate determination of power system frequency, and motor velocity. Some conditions such as oscillatory loads of motor/ or changes in motor load during a sampling period, and small changes in power system frequency may result in erroneous conclusions. Therefore, exact determination of supply frequency f and slip s, or velocity, is required. In [12], the authors introduced a method to obtain exact motor slip from a vibration spectrum. In the proposed method no pre-installed speed sensor is required. In [13] they have also shown that there are frequency components related to broken rotor fault in a vibration spectrum that were neglected in former works. A vibration sensor is the only required instrument in the proposed method.

Artificial Neural Networks (ANNs) have shown successful applications in motor fault diagnosis [14]-[17]. ANNs do not need a rigorous mathematical model for fault detection and they are very flexible in solving certain problems that have nonlinear complicated structures. In this work, a neural network broken rotor fault diagnosing system based on new features extracted from motor vibration spectrum is introduced. In the first part, the theoretical fundamentals will be presented, then some new features in vibration spectrum are introduced and the proposed method of extracting these features is explained. After a short introduction of the laboratory set, the vibration spectrums, and the vibration features obtained by the experimental tests are presented. Finally an explanation of the applied ANN concludes this paper.

2. Theoretical Fundamentals

2.1 Effects of broken bars on different motor signals

In a healthy 3-phase induction motor, each of the symmetrical currents in the stator and rotor produce a resultant forward rotating magnetic field at synchronous speed. If rotor asymmetry occurs - due to broken bars - then there will be a resultant backward rotating field at slip frequency sf with respect to the rotor. The backward rotating field of the rotor has the speed $-s\,f$ with respect to the rotor and $(1\text{-}s)\,f\text{-}sf = (1\text{-}2s)\,f$ with respect to the stator, where $(1\text{-}s)\,f$ is the forward rotor speed. Therefore, a current with the frequency $(1\text{-}2s)\,f$ is induced in the stator.

Interaction of the rotor backward rotating field with the forward stator field produces torque and velocity oscillations with the frequency of $2sf$. This oscillation acts as a frequency modulation on rotation frequency, as well as all slip-related frequency components in other machine signals. On the whole the following frequencies appear in different signal spectrums: $(1\pm2ks)f$ in stator current and instantaneous power, $(2k\text{-}1)sf$ in rotor current, $2ksf$ in velocity and torque, and ksf in axial flux, where k=1,2,3,… . These quantities can be obtained using different measuring sensors such as current clamps, searching coils, tachometers, etc.

2.2 Necessity of exact slip and power source frequency determination

The fault frequencies introduced in section 2.1 are slip and supply frequency dependent; therefore, in order to be detected in the related spectrum, the supply frequency and motor velocity should be known exactly, otherwise, the following conditions may result in erroneous conclusions:

- Small changes in power system frequency due to changes in power system load
- Motor load changes during test period
- Oscillatory loads of motor
- Existence of gearboxes in power transmission system
- Large motors, operating at small slips or at loads considerably less than nominal load
- Presence of other faults in motor or rotating system

When the frequency of a phenomenon changes, side band frequencies appear around the center frequency in the related spectrum. Thus, variation in power system frequency and motor speed produces extra frequencies. Oscillatory loads cause speed oscillations, and these oscillations create additional frequency components in different motor signals. These additional frequencies may be confused with broken rotor fault frequencies, especially when the motor operates at small slips. Other faults in the motor or rotating system produce their own frequency components, which may also be a cause for wrong diagnosis. Therefore, exact determination of supply frequency *f,* and slip or velocity is required. Also, none of the mentioned fault related frequencies can be evaluated without the aid of a speed measuring instrument, or an exact speed estimating system.

3. Proposed Method

3.1 Useful Features in Vibration Spectrum

One of the most essential steps in motor fault diagnosis is extraction of appropriate features from the motor signals so as to provide the classifier with distinguishable criteria for judgment on the input data. As explained in section 2-1, the existence of broken rotor bars causes some frequency components that can be used for fault detection. So the primary task is to locate the harmonics of interest in the frequency spectrum of machine's signal and to distinguish them from noisy or not fault related ones.

Classical on-line methods introduced in technical literature suffer from the deficiencies mentioned in section 1 and/or require an extra tool for speed measurement. In order to diagnose the motor condition a sample motor vibration by a suitable vibration sensor is proposed. Existence of rotor circuit asymmetry or broken bars produces certain frequency components in a vibration spectrum. These components are slip-dependent, but no speed sensor is required. Exact velocity and power source frequency can be found in the motor vibration spectrum and the slip value can be computed.

There is always some rotor mass asymmetry in a rotating system. Mass unbalance is a common cause of rotating machines vibration. To demonstrate the harmonic excitation effect of this unbalance, we considered the simple mass and spring system shown in Fig. 1-a. The system has one degree of freedom. The unbalance is defined by mass m situated at distance e from the geometric center of the shaft, rotating with velocity ω. The whole system mass- including m – is M. k and c are the stiffness and viscous damping terms, and x is the displacement relative to static equilibrium point. The dynamic equation of the system can be written as:

$$M\ddot{x} + c\dot{x} + kx = (me\omega^2)\sin\omega t \quad (1)$$

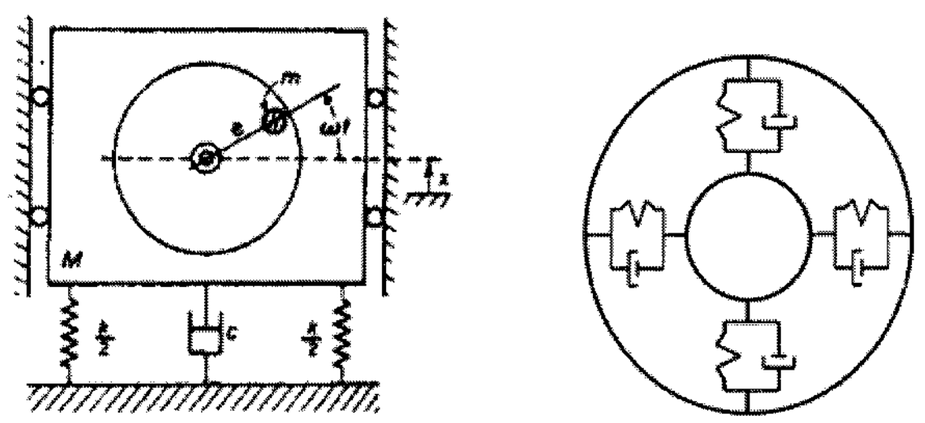

Fig. 1 a) Harmonic excitation due to rotating unbalance
b) Bearing model.

The steady state solution of this equation is a sinusoidal oscillation with frequency ω [18] - i.e. the rotation frequency appears in the vibration spectrum. The dynamic model of the induction motor rotor and the bearings is more complicated, but the results are the same. Fig. 1-b shows the dynamic model of a bearing [19]. The inner circle is the rotor shaft and the outer circle is the bearing housing. The system has two degrees of freedom. The centrifugal force due to rotor unbalance is transferred to the bearings and similar oscillations appear.

This mass unbalance together with a small probable misalignment between the motor shaft and load leads to strokes in different directions in each rotor revolution, these forces are periodic but are not sinusoidal, thus in addition to the frequency component at motor rotation speed f_m, its harmonics also appear in the vibration spectrum.

As mentioned in section 2.1, in the case of broken bars, there is a speed oscillation with frequency $2sf$. This oscillation acts as a frequency modulation on rotation frequency, thus the side band frequencies $f_m \pm 2ksf$ (where k= 1,2,3,…) appear around f_m in the vibration

spectrum. When the rotor circuit unbalance increases, the magnitude of speed oscillation as well as the magnitudes of the side band frequencies also increases. Therefore, the magnitudes of $f_m \pm 2ksf$ can be deemed proper measures for broken bar detection. Among these frequency components, $f_m \pm 2sf$ have the highest magnitudes and broken rotor bar fault can be better identified by them.

Since the frequency of the stator voltages and currents is *f*, the frequency of stator magnetizing currents and fluxes is f , too. The resultant flux that rotates at synchronous speed is independent of motor load and produces forces at twice power source frequency ($2f$). Therefore, this frequency is a strong component in the vibration spectrum.

The rotation frequency in an induction motor with *P* poles is a little smaller than *2f /P*. By searching the vibration signal spectrum, the exact mechanical frequency f_m and its harmonics can be determined. The frequency resolution Δf in a spectrum computed by FFT is reciprocal of sampling duration *T*. This resolution is constant all over the spectrum. Thus, it is better to consider higher order harmonics of velocity to determine slip more precisely. The *P*th harmonic of f_m is near and at the left side of $2f$ in the vibration spectrum and the exact slip can be given by

$$s = (2f - P f_m)/(2f) \tag{2}$$

Following the slip determination, the components related to rotor fault $f_m \pm 2sf$ can be found.

3.2 Determination of search intervals to find frequency components

FFT produces a spectrum composed of discrete frequency points with distances $\Delta f = 1/T$, where *T* is the sampling duration. Thus a frequency component f_o in the spectrum is located in the interval $f_o \pm \Delta f/2$. To find frequency components in equation (2) for computing motor slip, and then to determine the fault frequencies $f_m \pm 2sf$ in vibration spectrum, the error in extracting different frequencies should be evaluated and the search intervals should be determined.

The significant frequencies in the vibration spectrum are named below for ease of reference:

f_{ls}: fault related frequency $f_m - 2sf$, at left side of f_m

f_{rs}: fault related frequency $f_m + 2sf$, at right side of f_m

f_m : speed frequency in vibration spectrum

f_{mp} : *P*th harmonic of f_m in vibration spectrum

f_2 : twice power source frequency in vibration spectrum

Speed frequency f_m has the highest magnitude in a frequency range from nominal speed frequency to synchronous speed frequency *2f / P*. By determining f_m it is obvious that the speed frequency is within the interval $[f_m - \Delta f/2, f_m + \Delta f/2]$. Now f_{mp} and f_2 should be found. f_{mp} is corresponding to the highest amplitude in the interval $[Pf_m - P\Delta f/2, Pf_m + P\Delta f/2]$ and f_2 can be found in the vicinity of twice power supply frequency . The possible error in the value of determined f_{mp} and f_2 is $\pm \Delta f$. Now the motor slip can be determined by:

$$s = \frac{f_2 - f_{mp}}{f_2} \tag{3}$$

The turn computes the fault related frequencies. These quantities can be found by the following equations: f_{ls} can be found by:

$$f_{ls} = f_m - 2sf = f_m - (\frac{f_2 - f_{mp}}{f_2}) f_2 = f_m - f_2 + f_{mp} \tag{4}$$

f_{rs} can be found by:

$$f_{rs} = f_m + 2sf = f_m + (\frac{f_2 - f_{mp}}{f_2}) f_2 = f_m + f_2 - f_{mp} \tag{5}$$

By considering the error in determining f_{mp} , and f_2

$$\Delta f_2 = \Delta f_{mp} = \pm \frac{\Delta f}{2} \tag{6}$$

the maximum error in computing f_{ls}, and f_{rs} can be found by (4), (5), and (6):

$$\Delta f_{ls} = \Delta f_m \ - \Delta f_2 + \Delta f_{mp} = (\pm\frac{\Delta f}{2}) - (\pm\frac{\Delta f}{2}) + (\pm\frac{\Delta f}{2}) \quad (7)$$

$$\Delta f_{ls} = \pm\frac{3}{2}\Delta f$$

$$\Delta f_{rs} = \Delta f_m \ + \Delta f_2 - \Delta f_{mp} = (\pm\frac{\Delta f}{2}) + (\pm\frac{\Delta f}{2}) - (\pm\frac{\Delta f}{2}) \quad (8)$$

$$\Delta f_{rs} = \pm\frac{3}{2}\Delta f$$

(7) and (8) show that the fault frequency components should be within the intervals $f_{ls} \pm \frac{3}{2}\Delta f$ and $f_{rs} \pm \frac{3}{2}\Delta f$ respectively, with the highest magnitude in their relevant intervals. Since the border points may appear between two successive discrete frequencies, the search region should be extended to the neighboring points of these intervals. The feature extraction flow chart is shown in Fig. 2.

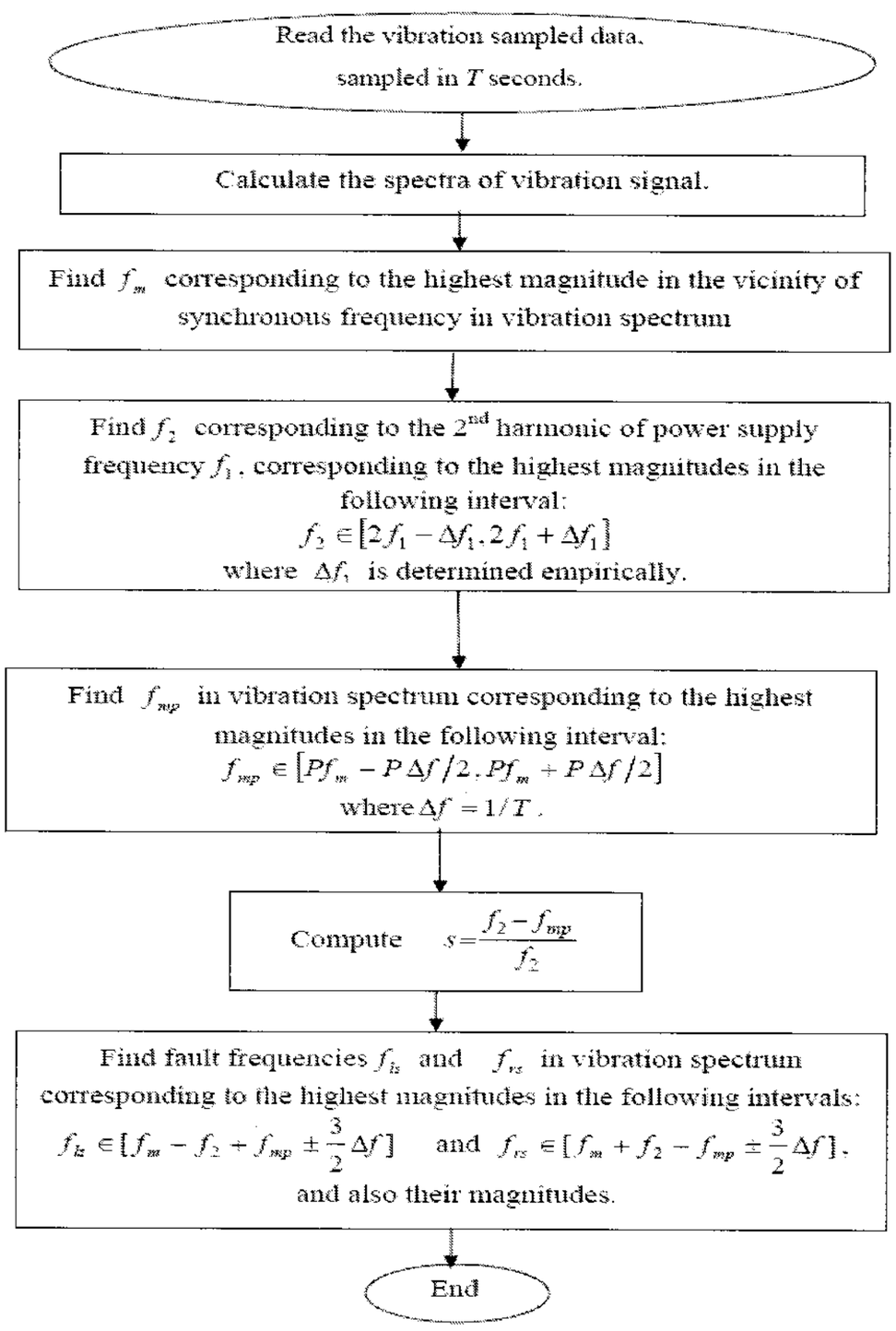

Fig. 2 The feature extraction flow chart

4. Test Setup

4.1. Practical notes on design and selection of test setup components

In order to evaluate motor signal spectrum, the signal obtained by a sensor should be amplified, filtered, and then sampled and quantized by a data logger to be used in a digital computer. Discrete Fourier Transform (DFT) is a useful method for identification of existing frequencies in a sampled signal. Algorithms for fast computation of DFT are called FFT.

To obtain the frequency spectrum of a signal, the following rules should be observed [20, 21]:

- Number of quantizing levels q, and the length of digital word n are related by $q = 2^n$. Each bit increment in word length, increases the signal to noise ratio by about 6 decibels. This note should be considered in data acquisition card selection.
- Based on the Nyquist sampling theorem, a band-limited signal $x(t)$ with no frequency component higher than f_h, can be uniquely determined by its samples if the sampling rate f_S is more than $2f_h$. The frequency $2f_h$ is commonly referred as the Nyquist sampling rate. If this rule does not hold, an overlap of spectrum repetition results in a distortion in the main signal spectrum, which is referred to as aliasing.
- In common practice, signals with unlimited band are passed through an anti-aliasing low-pass filter to eliminate unnecessary high frequencies before being sampled. Then the sampling frequency is chosen about ten times the cutoff frequency (the frequency in which the amplitude has dropped by 3 dBs). Otherwise existence of obtrusive frequencies results in unwanted aliasing.
- The Butterworth low-pass filter is a useful filter for the purpose of motor condition monitoring, because of its flat frequency response before cut-off frequency.
- Frequency resolution in signal spectrum Δf is reciprocal to sampling duration T. Both high sampling frequencies and long sampling durations increase the number of data points and the volume of

computations. Therefore, selection of T is based on a compromise between the expected precision and data logging system capabilities.

4.2. Test setup components

The test setup consists of a vibration sensor and its driver circuit, amplifier and filter circuit, data acquisition card, digital computer, related data acquisition and analysis software. The vibration sensor is an accelerometer, with a bandwidth of more than 10 kHz. The data acquisition card is a 16-bit card with a maximum sampling rate of 250 ks/s for all channels. The circuits consist of a current source to drive the vibration sensor and a low-pass 6th order Butterworth filter-amplifier with a cut-off frequency of 150Hz.

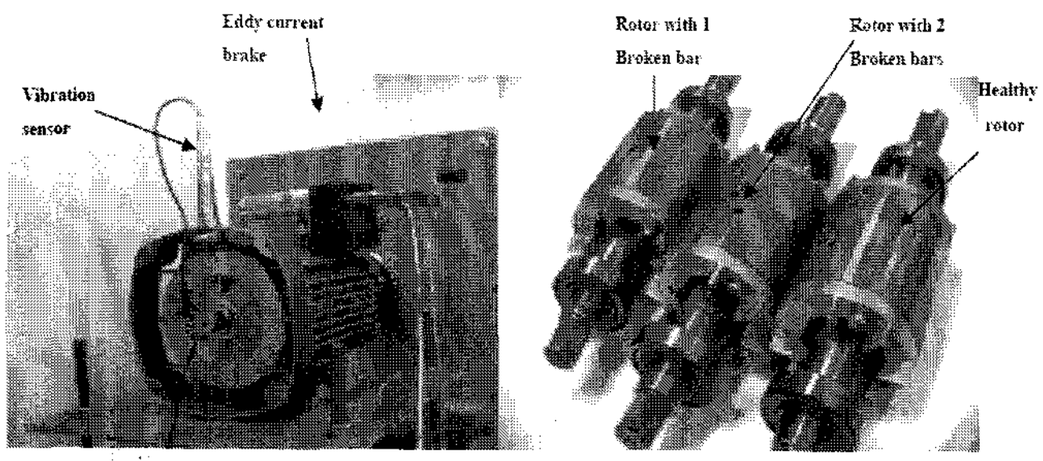

Fig. 3 Laboratory 3-phase, 380V, 4-pole, 50Hz, 1.1kW motor with one healthy and two defective rotors. The motor is connected to an eddy current brake

The test motor is a 3-phase, 380V, 4-pole, 50Hz, 1.1kW induction motor with two additional rotors. One of the rotors is healthy and the others have 1 and 2 broken bars respectively. The rotor bars are straight. The motor is connected to an eddy current brake load (Fig.3).

5. Experimental Results

Increasing the number of broken bars will increase the magnitude of fault sidebands – which appear in $f_m \pm 2sf$ frequencies. The correct place of these sidebands can be found by correct determination of supply frequency f, rotation frequency f_m, and slip s, which has been explained in section 3.2.

Due to limitation of available rotors, the tests were done on three rotors (one healthy, one with one broken bar, and one with two broken bars), but the results can be generalized to more broken rotors. It should be mentioned that in predictive maintenance of industrial applications, it is important to diagnose the first crack in the first bar in order to schedule a repair task and the designed system has this capability.

Numerous tests on the laboratory induction motor have been done at different levels of load from small slips to full load slips. In some cases, an oscillatory load was used. Speed frequency and its harmonics, second harmonic of power system frequency, and fault components have been determined carefully using feature extraction software based on the method introduced in section 3.

Fig. 4 shows a typical vibration spectrum of the tested laboratory motor with one broken bar. The sampling period in all the experiments shown in this paper have been 64 seconds and therefore the rotation frequency resolution is 1/64 Hz. All the vibration spectrums in this paper are normalized such that the main speed frequency components have 0 dB magnitudes. Figs. 4-b, and c show small portions of Fig. 4-a. It is seen that the desired frequency components can be distinguished easily, if the search region is known (as explained in section 3). The results obtained by the software are summarized in Table 1.

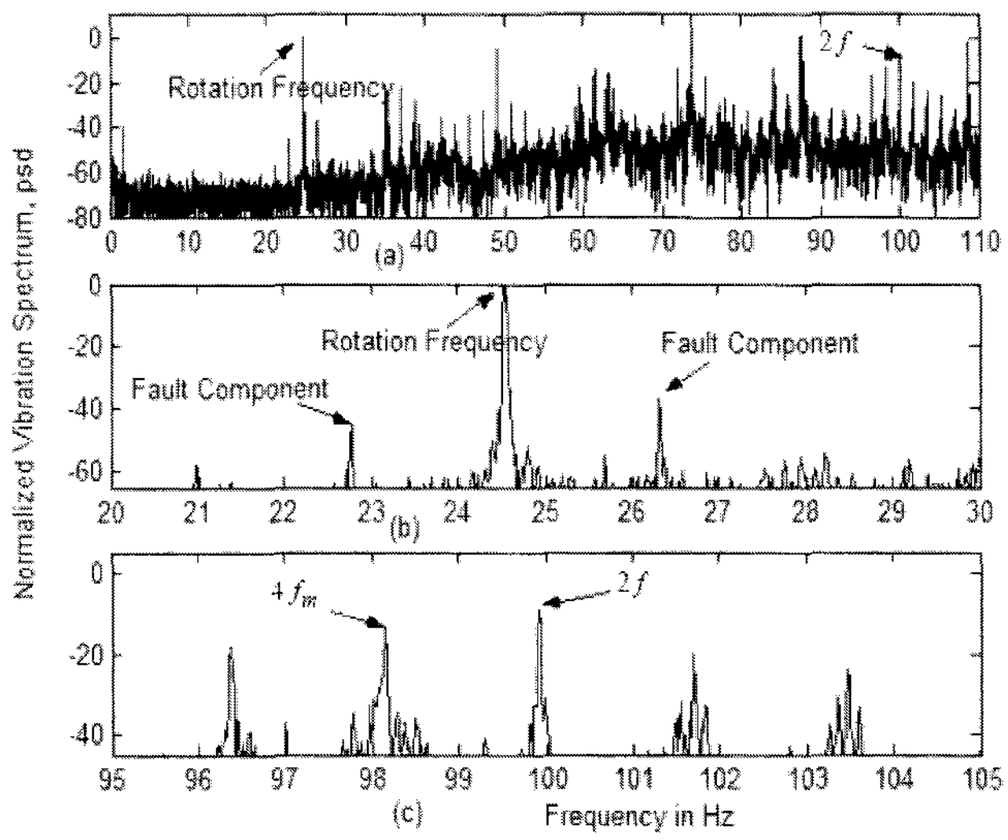

Fig. 4 Vibration spectrum of the 3-phase, 380 V, 4-pole, 50 Hz, 1.1 kW laboratory induction motor with 1 broken bar at 30% of nominal load. (a) Vibration spectrum. (b) Vibration spectrum in the vicinity of rotation frequency, showing the frequency components due to broken bar. (c) Vibration spectrum in the vicinity of 4th harmonic of rotation frequency and twice power system frequency

Table 1 Results extracted from vibration spectrum of Fig.4, laboratory motor at 30% of full load

Rotation frequency, f_m		24.53 Hz
4th harmonic of rotation frequency, f_{mp}		98.15 Hz
Twice network frequency, f_2		99.92 Hz
Slip computed by (3), s		0.0177
Fault component $f_m - 2sf$	Frequency	22.77 Hz
	Amplitude	-45.42 dB
Fault component $f_m + 2sf$	Frequency	26.31 Hz
	Amplitude	-36.65 dB

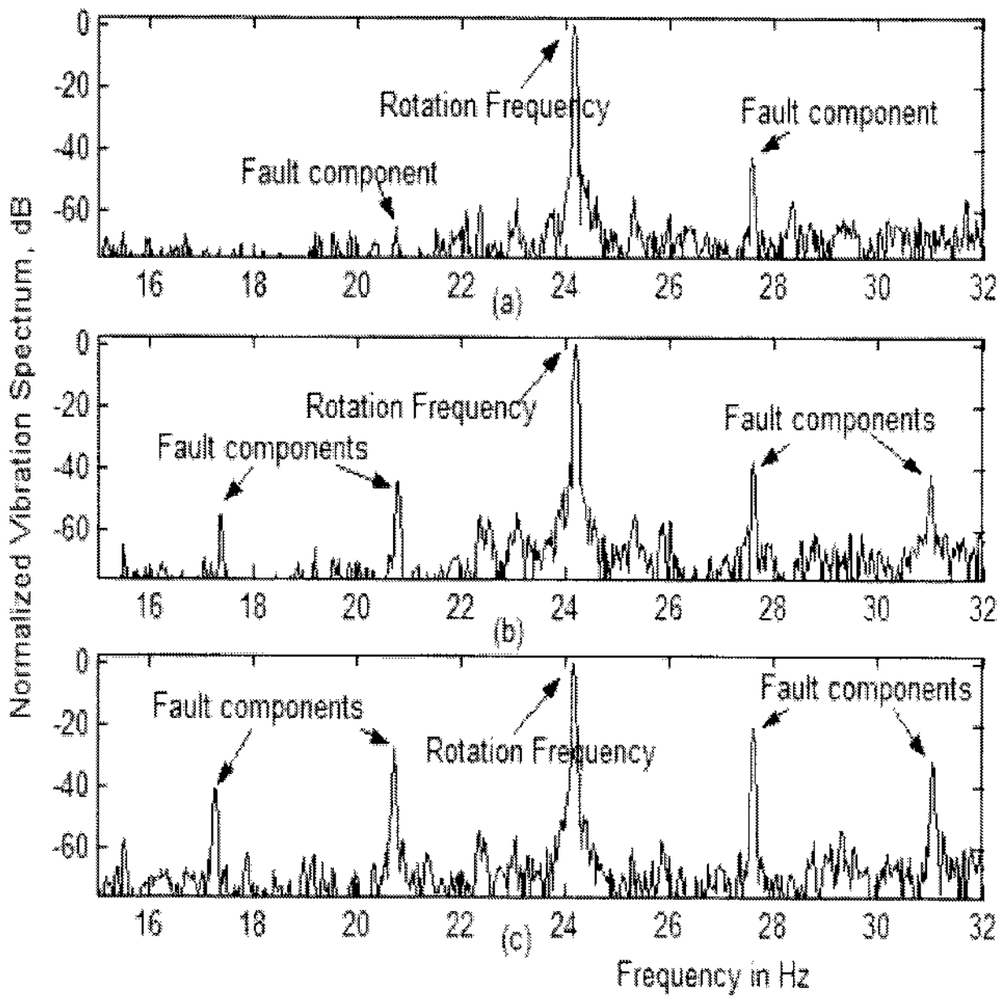

Fig. 5 Vibration spectrums of the 3-phase, 380 V, 4-pole, 50 Hz, 1.1 kW laboratory induction motor in the vicinity of rotation frequency. (a) Spectrum of motor with healthy rotor at 75% of nominal load . (b) Spectrum of motor with 1 broken bar in rotor at 65% of nominal load . (c) Spectrum of motor with 2 broken bars in rotor at 50% of nominal load . For equality of slips, motor loads are considered different intentionally

Fig. 5 shows the vibration spectrums of the laboratory motor with a healthy rotor (Fig. 5-a), with 1 broken bar (Fig. 5-b), and with 2 broken bars in the rotor (Fig. 5-c). A motor with broken bar operates at lower speeds as compared with the same motor with healthy rotor when the load torque is constant. Therefore, the load torques were intentionally considered differently, such that the slips are equal in Figs. 5-a, b, and c. This is seen in the fault extension has increased the magnitude of fault related frequencies;

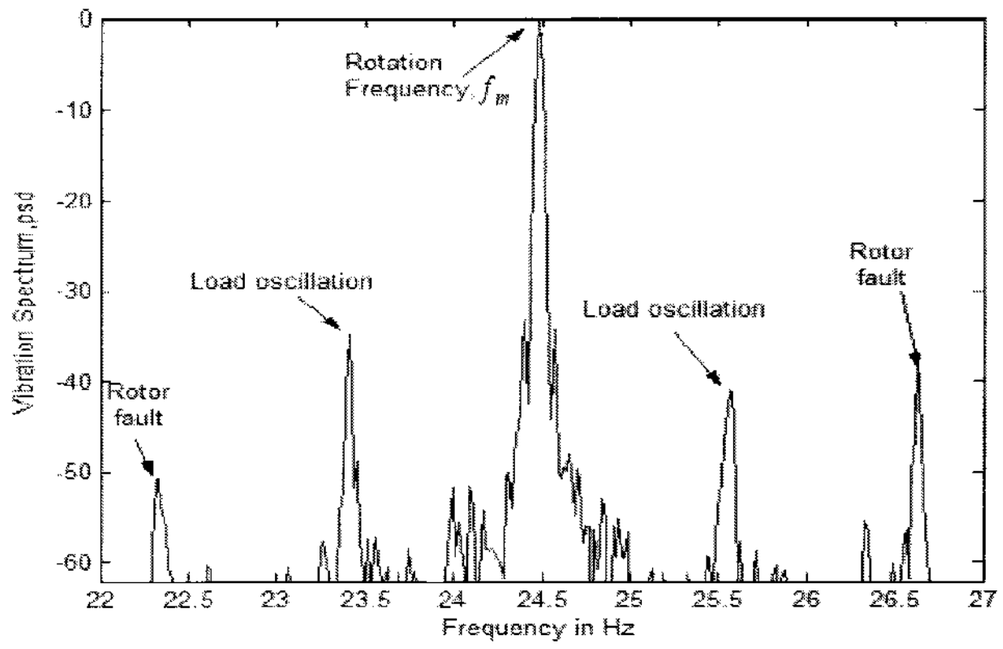

Fig. 6 Vibration spectrum of the 3-phase, 380 V, 4-pole, 50 Hz, 1.1 kW laboratory induction motor with 1 broken bar in the vicinity of rotation frequency. Motor load is oscillatory

therefore, evaluating the side band frequencies $f_m \pm 2sf$ in the vibration spectrum is an effective measure for broken rotor fault diagnosis. Fault related frequencies and amplitudes of motor in Fig. 5 are determined by the method described in section 3 and the results are listed on Table 2. Although the loads were different, the slips were equal (0.034 in all three experiments).

Fig. 6 shows the vibration spectrum of the motor with 1 broken bar in the rotor and oscillatory load. Load oscillation has been produced by injecting an oscillatory current to the eddy current brake circuit. The frequency of load oscillation is about 1 Hz. Frequency components related to rotor asymmetry or broken bar, as well as frequencies related to load oscillations are shown by arrows. Failing to distinguish between these components may result in erroneous evaluation of motor condition. By using the search intervals introduced in section 3.2 there is no confusion in distinguishing fault frequencies.

The variations of fault components magnitudes versus slip are shown in Fig. 7. This diagram is obtained by achieving numerous experiments on the laboratory motor with healthy and defective rotors at different loads from 25% to 110% of nominal load. 10% of loads have been oscillatory. The vibration spectrums amplitudes have been normalized (as mentioned before), and a computer program has obtained the magnitudes of fault related

Table 2 Amplitudes and frequencies of fault related components extracted from vibration spectrum of Fig. 5

		Motor with healthy rotor at 75% of nominal load, s= 0.034	Motor with 1 broken bar in rotor at 65% of nominal load, s= 0.034	Motor with 2 broken bars in rotor at 50% of nominal load, s= 0.034
Fault component $f_m - 2sf$ in vibration signal	Frequency	20.7 Hz	20.7 Hz	20.7 Hz
	Amplitude	-65.4 dB	-43.6 dB	-27.4 dB
Fault component $f_m + 2sf$ in vibration signal	Frequency	27.6 Hz	27.6 Hz	27.6 Hz
	Amplitude	-42.5 dB	-37 dB	-20.6 dB

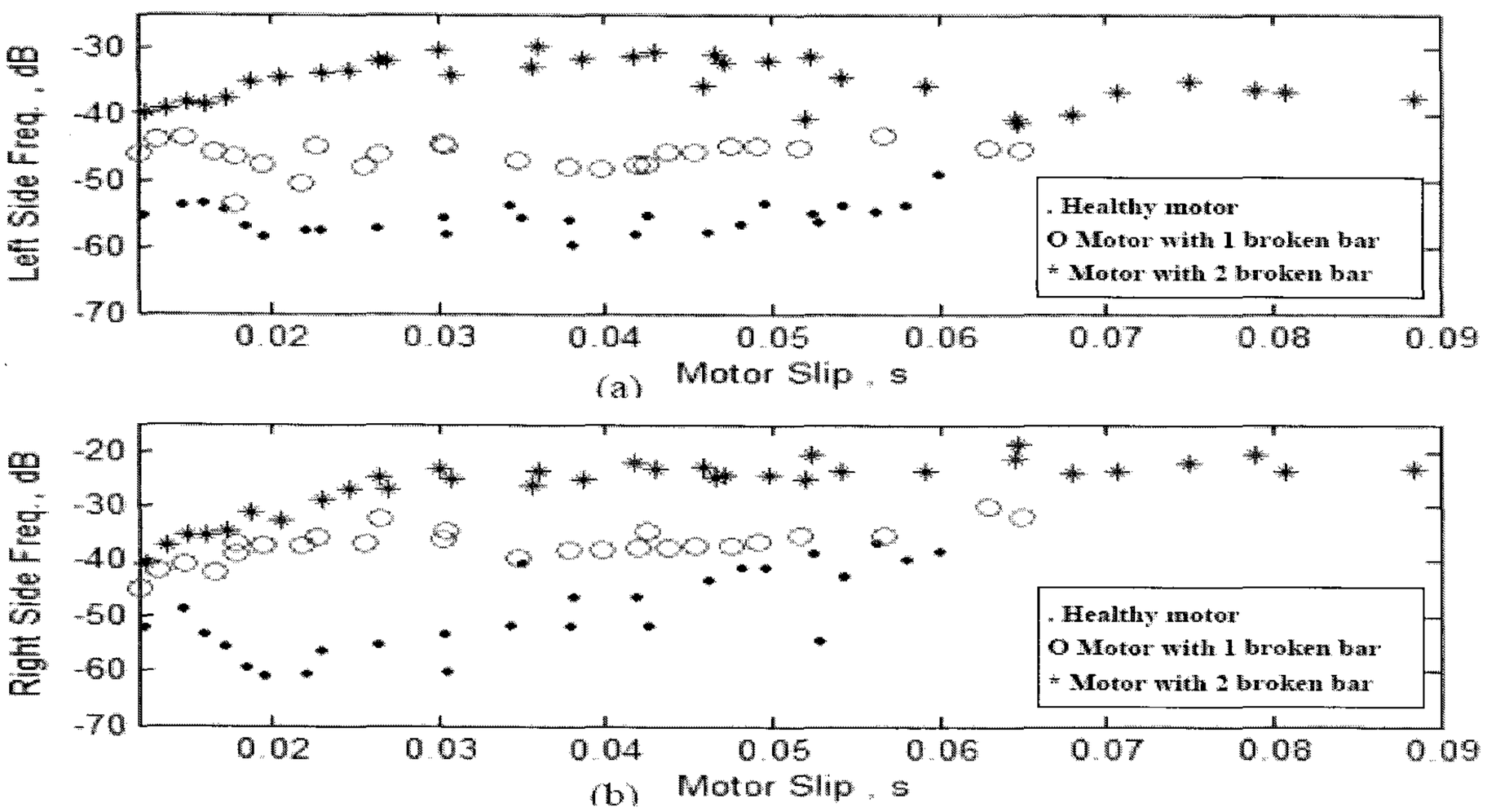

Fig. 7 Normalized amplitudes related to broken rotor fault versus slip, for motors with healthy rotor, 1 broken bar, and 2 broken bars. (a) Variations of the fault component at the left side of rotation frequency, f_{ls} . (b) Variations of the fault component at the right side of rotation frequency, f_{rs}

components $f_m \pm 2sf$ (or f_{ls} and f_{rs}) by using the method introduced in section 3.

Fig. 7 shows that; at least one of the amplitudes of fault components in healthy and defective cases differs. Furthermore, it is observed that the points related to defective rotors have spread toward higher slips. These variations though a logical trend but are nonlinear and complicated. Judgment of these variations requires an expert person. Neural networks can replace the expert person and improve the fault detection rate.

Therefore, if there is enough training data, an artificial neural network can be a suitable candidate for fault diagnosis.

In small slips, due to variations of network frequency and load, as well as other obtrusive factors, neighboring frequency components are combined and the resultant amplitude does not show the motor condition exactly. The situation can be improved by prolonging vibration sampling duration and increasing frequency resolution in the vibration spectrum.

5.1 The Applied Neural Network Structure

Neural networks use a dense interconnection of computing nodes to approximate nonlinear functions

[22]-[23]. Each node constitutes a neuron and performs the multiplication of its input signals by constant weighing, summing up the results and mapping the sum to a nonlinear activation function φ; the results are then transferred to its output. A feed-forward ANN is organized in layers: an input layer, one or more hidden layers, and an output layer. The mathematical model of a neuron is given by:

$$y = \varphi\left(\sum_{i=1}^{N} w_i.x_i - b\right); \tag{9}$$

where: (x_1, x_2, ...,x_N) are inputs from the previous layer neurons, (w_1, w_2, ...,w_N) are the corresponding weights and, b is the bias of the neuron. φ is generally a nonlinear function. The ANN is trained by a learning algorithm that performs the adaptation of weights of the network.

This study uses MLP (multi layer perceptron) three layer feed forward neural networks in a Matlab environment. The network is fully connected, i.e., the output of each neuron is connected to all the neurons in the forward layer through a weight. The functions applied in hidden layer and output layer are tangent hyperbolic (tansig) given by:

$$\varphi(x) = \frac{1 - e^{-2x}}{1 + e^{-2x}}$$

and logarithmic sigmoid (logsig) given by:

$$\varphi(x) = \frac{1}{1 + e^{-x}}$$

respectively, where $x = \left(\sum_{i=1}^{N} w_i.x_i - b\right)$ as mentioned in (9).

The number of neurons in hidden layer was selected by trial and error. There is no precise method to select the number of these neurons. The structure of the proposed feed-forward neural network is indicated in Fig. 8. The ovals in the network represent the neurons.

The input vector of the neural network consists of the magnitudes of two side band fault frequency components (f_{ls} and f_{rs}), and motor slip s. The network has three outputs which in each case of healthy rotor, rotor with one broken bar, and rotor with two broken bars, one of the outputs is "1" and the others are zero. Different numbers of hidden neurons were tried in order to select an optimum one. The procedure is explained in the next section.

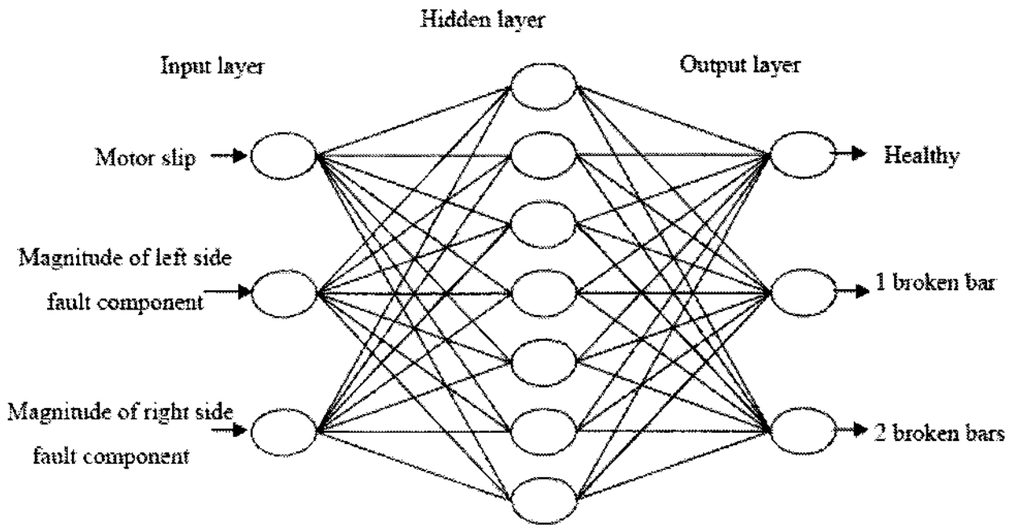

Fig. 8 Topology of the neural network for broken rotor fault diagnosis

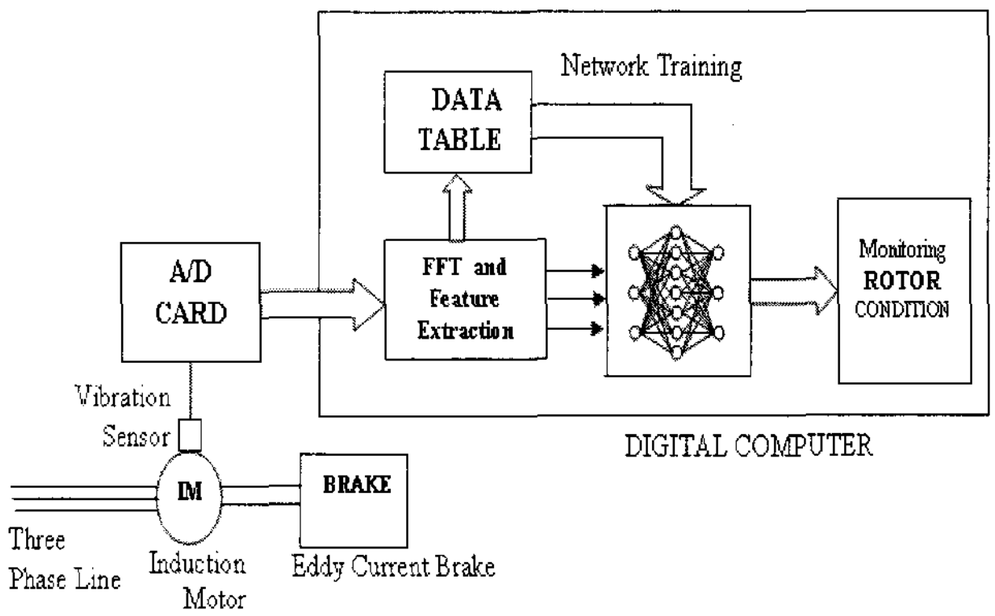

Fig. 9 Broken bar fault diagnosing system: software and hardware

5.2 Training and Test Procedure

The training and test procedure used in the present research is illustrated in Fig. 9. The feature extraction software generates the input/output data vectors for different vibration signals obtained from different experiments. The input data corresponds to the magnitudes of side band fault components and slip. The output data corresponds to the actual rotor condition, i.e., a vector with two "zeros" and one "1." These vectors are collected in a data table.

Several tests were done for different levels of loads, and their related vectors were obtained. The total number of vectors is 120 (40 for a healthy motor, 40 for a rotor with 1 broken bar, and 40 for a rotor with 2 broken bars).

In the learning procedure, random weights were initially assigned to the network and the learning rule used was Levenberg-Marquardt. The network has three layers with three inputs and three outputs. To determine the number of

neurons in a hidden layer and to train the network the following procedure is done:

a. Choose the number of neurons in the hidden layer (a number between 5 and 50).
b. Select 60 vectors from the data table at random for network training.
c. Activate the network learning step.
d. Test the network performance with the remaining data vectors, and specify the percentage of correct diagnosis.
e. To evaluate the reliability of the chosen number for neurons in the hidden layer, repeat steps b, c, and d 30 times. Then write the minimum, maximum, and average percentage of correct diagnosis in a table.
f. Repeat the above steps (a-e) for a new number of neurons in the hidden layer.

The minimum, maximum, and average percentages of correct diagnosis for some of the hidden layer neurons are shown in Table 3. The results show that by 25 the number of neurons in a hidden layer is the highest percentage of correct diagnosis obtained, so it is the best choice and the method is reliable.

The ability of the neural network to diagnose the motor condition is demonstrated more accurately if the number of test experiments is increased. By considering this rule, one of the trained ANN's with 25 hidden layer neurons was used in a laboratory by an examiner with no former knowledge about the motor condition, and in all cases the motor condition was diagnosed correctly.

Table 3 Results of correct diagnosing percentage for different number of neurons

Number of Neurons	min	max	average
15	86	100	96
25	91	100	98
35	89	100	96

6. Conclusion

In this paper an intelligent broken rotor fault diagnosing method was introduced. The method applies new features extracted from a motor vibration spectrum to train an MLP feed forward neural network. A vibration sensor is the only necessary sensor and this method needs no knowledge of motor structure (other than number of poles). The proposed method is able to distinguish between fault and not- fault frequency components. According to the proposed method, a fault-diagnosing instrument was successfully designed. Tests on laboratory motors have proved the efficiency of this method, so that a person with no former knowledge about motors will be able to correctly diagnose the motor's condition in all cases.

References

[1] Benbouzid M.E.H., "A review of induction motors signature analysis as a medium for fault detection", *IEEE Trans.Ind Electron.*, Vol. 47, No. 5, pp. 984-993, Oct. 2000.

[2] Nandi S., Toliyat H., Li X., "Condition monitoring and fault diagnosis of electrical motors-a review", *IEEE Trans. Energy Convers.*, Vol. 20, No. 4, pp. 719–729, Dec. 2005.

[3] Elkasabgy N. M. ,Eastham A. R.,Dawson G.E., "Detection of broken bars in the cage rotor on an induction machine", *IEEETrans.Ind.Applns.*,Vol. IA-22, No.6, pp.165-171, 1992.

[4] Deleroi W., "Squirrel cage motor with broken bar in the Rotor –Physical Phenomena and their experimental assessment", *ICEM,* Budapest, pp. 767-770, 1982.

[5] Filippetti F., Franceschini G. ,Tassoni C.,Vas P., "A technique in induction machines diagnosis including the speed ripple effect", *IEEE – IAS annual Meeting Conference*, San Diengo, pp. 655-662, Oct 6-10,1996.

[6] Cardoso A. J. M., Crus S. M. A., Carvalho J.F.S., Saraiva E. S., "Rotor cage fault diagnosis in three phase induction motors, by Park's vector approach", *IEEE IAS 95*, pp. 642-646, 1995.

[7] Gaydon B.G., "An instrument to detect induction motor rotor circuit defects by speed fluctuation measurements", *Electric Test and Measuring Instrumentation, Testmex 79 Conference Papers,* pp. 5-8, 1979.

[8] Legowski S.F.,Trzynadlowski A., "Instantaneous stator power as a medium for the signature analysis of induction motors", *IEEE IAS9*, pp. 619-624, 1995.

[9] Liu Z., Yin X., Zhang Z., Chen D., ChenW., "Online rotor mixed fault diagnosis way based on spectrum analysis of instantaneous power in squirrel cage induction motors", *IEEE Trans. on Energy Conversion,* Vol. 19, No. 3, pp. 485-490, 2004.

[10] Kliman G. B., Stein J. Endicott R. D., Madden M. W., "Non-invasive detection of broken rotor bars in operating induction motors", *IEEE Trans. Energy Conversion*, Vol. EC-3, No. 4, pp. 873-879, Dec. 1998.

[11] Bellini A., Filippetti F., Franceschini G., Tassoni C.,

Kliman G., "Quantitative evaluation of induction motor broken bars by means of electrical signature analysis", *IEEE Trans. Ind. Applications*, Vol. 37, No. 5, pp. 1248-1255, Sep/Oct. 2001.

[12] M. Ebrahimi, A. Sadoughi, M. Bayat, "Induction motor broken bar diagnosis by simultaneous current and vibration sampling", *XVII International Conference on Electrical Machines, ICEM2006*, Greece. Sept. 2006.

[13] A. Sadoughi, M. Ebrahimi, E. Rezaei, "A New Approach for Induction Motor Broken Bar Diagnosis by Using Vibration Spectrum", *SICE-ICASE International Joint Conference 2006*, Bexco, Busan, Korea, pp. 4715-4720, Oct. 18-21, 2006.

[14] M. Rokonuzzaman and M.A. Ranman, "Neural network based incipient fault detection of induction motors", *IEEE-IAS*, pp. 199-202, 1995.

[15] F. Filippetti and G. Franceschini, "Neural networks aided on-line diagnostics of induction motor rotor faults", *IEEE Trans. On Industry Applications*, Vol. 31, No. 4, pp. 892-899, Jul./Aug. 1995.

[16] M.Y. Chow, "Design considerations for a motor fault detection artificial neural network", *IEEE, Industrial Electronics, Control, Instrumentation, and Automation Conference*, Vol. 3, pp. 1455-1459, Nov. 1992.

[17] M. Moradian, M. Ebrahimi, M. Danesh, and M. Bayat, "Detection of broken bars in induction motors using a neural network", *Journal of Power Electronics, Korean Institute of Power Electronics,* pp. 245-252, July 2006.

[18] Thomson w. T., Dahlieh M. D., *Theory of Vibration with Applications*.

[19] Lalanne M., Ferraris G., *Rotordynamics Prediction in Engineering*, 2nd edition, John Wiley and Sons, 1998.

[20] Oppenheim A. V., Schafer R.W., *Discrete – Time Signal Processing*, Prentic-Hall, 1989.

[21] Willi ams A.B., Taylor F.J., Electronic Filter Design Hand Book, 3rd ed., 1995.

[22] Kartalopoulos S. V., Understanding Neural Networks and Fuzzy Logic- Basic Concepts and Applications, IEEE press, 1996.

[23] Menhaj M. B., *Computational Intelligence (vol.1), Fundamentals of Neural Networks*, Amirkabir Univ. Press, 2000.

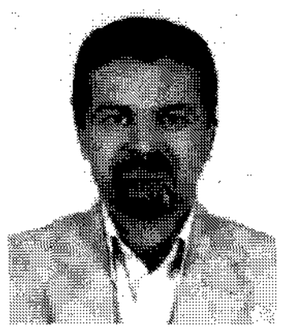

Alireza Sadoughi was born in Bandarabbass, Iran, in 1962. He received his B.S. and M.S. degrees in electrical engineering from Tehran University in 1987 and 1989, respectively. He has been a Faculty Member of Shahid-Chamran University and Malek-Ashtar University of Technology. Currently, he is a Ph.D. candidate in the Department of Electrical Engineering, Isfahan University of Technology, Isfahan, Iran. His research interests include electrical machines analysis and design, condition monitoring and fault diagnosis of electric machines and rotating systems, and simulation techniques in electrical machines.

Mohammad Ebrahimi was born in Isfahan, Iran, in 1958. He received his B.S. and M.S. degrees in electrical engineering from Tehran University in 1984 and 1986, respectively, and received his Ph.D. degree in 1996. He is an Assistant Professor in the Department of Electrical Engineering, Isfahan University of Technology, Isfahan, Iran. His research interests include application of artificial intelligence based electrical machines and derives, sensorless electric motor drives, condition monitoring and fault diagnosis of electric machinery, simulation techniques in electrical machines and derives, efficiency optimization and energy saving.

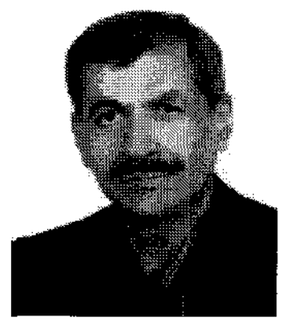

Mehdi Moallem (SM IEEE'90) received his Ph.D. degree in electrical engineering from Purdue University, West Lafayette, IN, in 1989. He is currently a full Professor with the Department of Electrical and Computer Engineering, Isfahan University of Technology, Isfahan, Iran. He has authored many journals and conference papers. His research interests include design and optimization of electromagnetic devices, application of advanced numerical techniques and expert systems for analysis and design of electrical machines, fault diagnosis, and power quality.
Prof. Moallem is a recipient of many international and national awards.

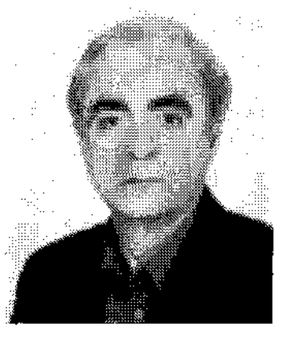

Saeid Sadri was born in Isfahan, Iran. He received his Ph.D. degree in electrical engineering from the Department of Electrical Engineering, Isfahan University of Technology, Isfahan, Iran in 1999 where he is an Assistant Professor. His research interests include signal processing, and application of artificial intelligence in signal processing. He has authored many papers and conducted much research in these fields.